

Segmentation of Histopathological Images with LinkNet Model Supported by Vgg16 Backbone

Furkan ATLAN^{1*} 

¹Department of Management Information Systems, Burdur Mehmet Akif Ersoy University, Burdur, Türkiye

ABSTRACT

Nuclei segmentation in histopathological images is crucial for the processing and analysis of medical images. Manual segmentation of nuclei images is challenging due to subjective errors by experts and image noise. Before the use of artificial intelligence in medical image analysis, segmentation tasks were performed with common classical methods such as thresholding and watershed. The development of deep learning has led to the emergence of models specifically designed for segmentation tasks. In this study, LinkNet model supported with Vgg16 backbone is proposed for segmenting histopathological images in CryoNuSeg dataset created for nucleus segmentation. After a small number of images are multiplied with data augmentation, feature maps are generated using the Vgg16 model integrated into the encoder of the LinkNet architecture. The results obtained in this study, with F1 Score, Intersection over Union (IoU), and Aggregated Jaccard Index (AJI) values of 0.8447, 0.7312, and 0.7312 respectively, demonstrate superior performance compared to recent studies utilizing the same dataset.

Keywords: Medical image segmentation, CryoNuSeg, Backbone, Vgg16, LinkNet

1. INTRODUCTION

Histopathology is the microscopic examination of tissue samples to detect structural abnormalities and pathological changes, serving as a cornerstone of disease diagnosis, particularly in oncology. In clinical practice, pathologists analyze stained tissue sections—typically prepared with Hematoxylin and Eosin (H&E)—to identify disruptions in tissue architecture, variations in nuclear morphology, and the presence of inflammatory or malignant cells. This process, although vital for determining disease stage and guiding treatment, is labor-intensive and subject to inter-observer variability. Recent advances in digital pathology and computational image analysis have transformed histopathology into a data-rich domain, allowing whole-slide images (WSIs) to be assessed algorithmically. In this context, deep learning-based approaches, often referred to as computational pathology (CPATH), have shown great potential in automating diagnostic workflows, improving reproducibility, and addressing the global shortage of expert pathologists [1].

Digital pathology enables the extraction of information from stained and digitized tissue samples obtained from patients. This information is shared and managed among experts, thereby providing benefits such as allowing remote specialists to interpret these images or utilizing samples for scientific research [2]. Additionally, digitized images can also be employed for computer-aided quantitative image analysis [3]. Performing image analysis in digital pathology supported by artificial intelligence raises expectations of significantly improving clinical applications [4].

Examination of tissue sections stained with H&E provides valuable insights into cells and their functions [5]. This is because H&E-stained tissue images play a crucial role in diagnosing various cancer types, including breast, prostate, and liver cancers. Factors such as shape, type, morphology, density, and quantity of nuclei are fundamental components in the evaluation of H&E-stained tissue images [6].

Nuclei segmentation is biologically crucial, as information extracted from tissue images enables observations regarding cell cycles and mutations in cancer-related proteins, thereby facilitating the advancement of research. However, challenges exist in nuclei segmentation due to factors such as noise in images, overlapping of cells, and complications arising during manual preparation processes [7-8].

*Corresponding Author Email: fatlan@mehmetakif.edu.tr

Submitted: 16.03.2025 Revision Requested: 07.04.2025 Last Revision Received: 02.05.2025

Accepted: 06.05.2025 Published Online: 22.05.2025



Burdur
Mehmet Akif Ersoy
University Press



Cite this article as: Atlan, F. (2025). Segmentation of Histopathological Images with LinkNet Model Supported by Vgg16 Backbone. Scientific Journal of Mehmet Akif Ersoy University, 8(1): 35-46.

DOI: <https://doi.org/10.70030/simakeu.1658832>

<https://dergipark.org.tr/simakeu>



Content of this journal is licensed under a Creative Commons Attribution-NonCommercial 4.0 International License.

Manual segmentation is considerably costly due to factors such as the necessity for clinical expertise, the time-consuming nature of the task, and susceptibility to human error. Consequently, automated nuclei segmentation methods have been developed to reduce workload and establish models with the highest possible accuracy.

The initial models developed for automated nuclei segmentation mainly consisted of watershed segmentation, morphological operations, and thresholding methods. However, these classical approaches had several disadvantages, including the requirement for manual parameter tuning, limited generalizability across multiple organs and tissue types, and reduced performance in the presence of noise [9]. Following the availability of large annotated datasets and the success of deep learning models such as Convolutional Neural Networks (CNNs), the use of classical methods in automated nuclei segmentation tasks has progressively declined. Instead, models employing Fully Convolutional Networks (FCNs) have become more favorable [10]. FCN architectures typically consist of encoder-decoder blocks, which often exhibit symmetrical structures. Specifically, within medical image segmentation, the most popular FCN-based architecture is the U-Net model [11]. Upon recognition of the significance of nuclei segmentation, state-of-the-art models and their modified versions have emerged in this field. Examples of such advanced models include U-Net++ [12] and 3D U-Net [13].

Accurate decoding of features learned by the encoder at higher resolutions in the decoder is essential for automated nuclei segmentation. For this reason, proven deep learning architectures can be used as "backbones" in encoder sections instead of relying solely on the layers of the original model [14-16].

The objective of this study is to automate nuclei segmentation by utilizing the Vgg16 model [17] as the backbone structure of LinkNet [18], a Fully Convolutional Network (FCN) architecture specifically developed for segmentation tasks. The choice of the LinkNet model instead of the widely adopted U-Net architecture, which is extensively used in medical image segmentation, stems from the hypothesis that employing state-of-the-art architectures as backbones within segmentation models—rather than relying on their original internal layers—may yield superior performance. Here, the primary focus is placed upon the potential improvement in segmentation accuracy achievable by integrating more effective models within the encoder section. In other words, the emphasis is on evaluating the influence of the backbone model rather than the segmentation architecture itself. Consequently, the LinkNet model was preferred over the conventional U-Net.

This study is organized as follows: Section 2 presents the relevant literature. The dataset is described in Section 3. Methodology is provided in Section 4. System details are discussed in Section 5. Section 6 presents the results of the study. Section 7 concludes the paper.

2. LITERATURE REVIEW

Deep learning-based models play a crucial role in nuclei segmentation. Table 1 provides an overview of the literature on nuclei segmentation.

Table 1. Literature review on nuclei segmentation in histopathological images

Author(s)	Methodology	Dataset	Metrics			
			DCS	F1-Score	IoU	AJI
[19]	Enhanced U-Net with deeper encoder layers	Data Science Bowl	-	-	0.567	-
[20]	Residual + Bottleneck + Attention-based Decoder	Kumar [21]	-	0.811	0.685	-
[22]	Multi-task, 3-branch U-Net with region enhancement	ConSep	0.854	-	-	0.561
		CPM17	0.884	-	-	0.712
[23]	U-Net with ResNet encoder	PanNuke	-	0.841	-	0.740
[24]	Vision Transformer-based model with multi-scale encoding	GCNS	0.725	-	-	-
[25]	Dense conv + normalization + local & global feature fusion	PanNuke	0.865	-	0.844	-
		ConSep	0.844	-	0.823	-
[26]	U-Net with VGG16 encoder	MoNuSeg	-	0.845	0.693	-

In this study, a LinkNet segmentation model supported by a VGG16 backbone is proposed for nuclear segmentation, in which the VGG16 model serves as the encoder. The primary distinction of the proposed method from other conventional encoder-based models lies in the preprocessing of images before being fed into the model. Here, the proposed approach is not only a model but a comprehensive framework that incorporates image preprocessing prior to segmentation. The effectiveness of the proposed method was evaluated on histopathological images from the CryoNuSeg dataset, yielding successful results.

3. DATASET

3.1. CryoNuSeg Dataset

The CryoNuSeg dataset [27] consists of 30 histopathological images stained with H&E, representing ten different organs, each with a resolution of 512×512 pixels. Figure 1 shows nuclei images of different organs in the CryoNuSeg dataset.

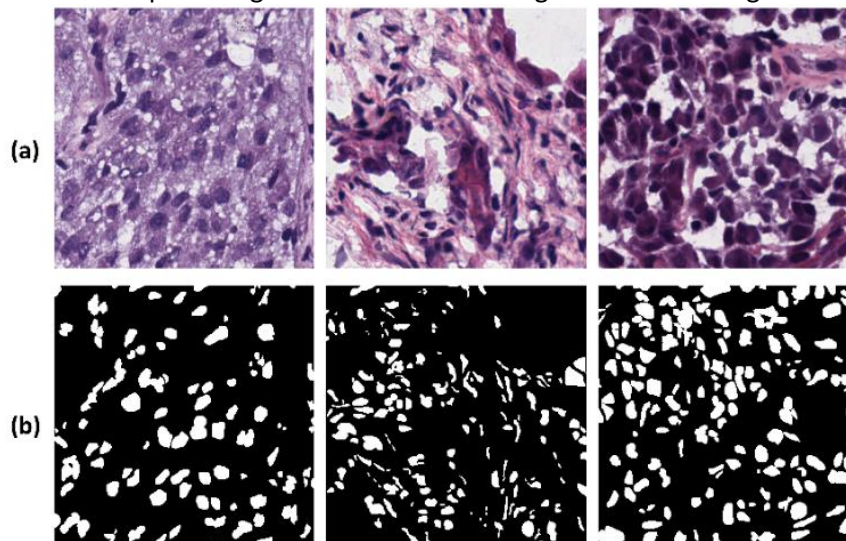


Fig 1. Examples from the CryoNuSeg dataset (a) Organ images, (b) Segmentation masks (From left to right: adrenal gland, pancreas, and skin images.)

Table 2 presents the descriptive statistics of the dataset, while Figure 1 illustrates example images from the CryoNuSeg dataset.

Table 2. Descriptive Statistics of the CryoNuSeg Dataset

Organ	Number of Images	Number of Nuclei
Adrenal gland	3	344
Thyroid gland	3	464
Pleura (Lung membrane)	3	515
Lymph node	3	1308
Testis	3	793
Skin	3	436
Thymus	3	1646
Pancreas	3	548
Mediastinum	3	1349
Larynx	3	641
Total	30	8044

3.2. CPM-17 Dataset

The CPM-17 [28] dataset, provided as part of the MICCAI 2017 Digital Pathology Challenge, comprises a total of 64 histopathological images—32 for training and 32 for testing—each with a resolution of 500×500 pixels, including 7,570

annotated nuclei. In this study, the proposed model, initially trained on the CryoNuSeg dataset, was evaluated on the 32 test images from the CPM-17 dataset.

4. METHODOLOGY

4.1 Data Preprocessing

Data augmentation was applied to the 30 images in the dataset. Data augmentation is a common regularization technique in deep learning [29]. When the number of training images is limited, increasing the dataset size enhances data diversity and improves model learning, making it a preferred preprocessing approach [30].

Flipping and cropping data augmentation techniques were applied to 25 training images. In the flipping technique, images were mirrored along the x-axis, y-axis, and both axes. In the cropping technique, images were randomly cropped within a range of pixel values. As a result of applying these two augmentation techniques, resulting in a total of 1,000 augmented training images.

4.2 LinkNet

LinkNet is a semantic segmentation model consisting of a total of eight blocks, including four encoder and four decoder blocks. On the encoder side, a convolution operation is first performed using a 7×7 matrix, followed by max pooling over a 3×3 region. Batch normalization [31] is applied between each convolutional layer, followed by the nonlinear ReLU activation function [32]. The convolution process in the encoder begins with 64 feature maps, and through downsampling, the number of feature maps doubles at each stage, reaching 512 in the final encoder block. In the decoder part, the 512 feature maps undergo upsampling to restore the resolution, and at each stage, the number of feature maps is reduced by half. By the time the process reaches the first block, the segmentation is completed with 64 feature maps, matching the initial configuration.

4.3 Vgg16

VGG16 is a deep learning model consisting of five convolutional blocks, each containing a max pooling layer. The first two convolutional blocks include two convolutional layers followed by a max pooling layer, while the remaining three convolutional blocks contain three convolutional layers and a max pooling layer [33]. The first convolutional block utilizes 64 filters, and the number of filters doubles at each subsequent block until the fifth block, where 512 filters are maintained, as in the previous block. Finally, the model is completed with three fully connected layers, followed by the softmax activation function [34].

4.4 Metrics

The performance of the proposed model was evaluated using the Dice Coefficient Score (DCS), F1-score, Intersection over Union (IoU), and Aggregated Jaccard Index (AJI) metrics. These metrics are widely utilized in segmentation studies to assess the effectiveness of the segmentation process by quantifying the similarity between predicted and ground truth masks.

The mathematical formulations of the DCS, F1-score, IoU, and AJI metrics are presented in Equations 1–4, respectively.

$$DCS = \frac{2 * |t \cap \hat{t}|}{|t + \hat{t}|} \quad (1)$$

In Equation 1, t represents the ground truth segmented nucleus, while \hat{t} denotes the nucleus obtained as a result of the prediction.

$$F1 \text{ Score} = 2 * \frac{\text{Recall} * \text{Precision}}{\text{Recall} + \text{Precision}} \quad (2)$$

$$IoU = \frac{TP}{TP + FP + FN} \quad (3)$$

In Equation 3, TP refers to True Positive, FP represents False Positive, and FN denotes False Negative values.

$$AJI = \frac{\sum_{i=1}^{n_0} |G_i \cap S(G_i)|}{\sum_{i=1}^{n_0} |G_i \cup S(G_i)| + \sum_{k \in K} |S_k|} \quad (4)$$

In Equation 4, $n\varrho$ represents the number of segmented nuclei, G_i denotes the set of segmented nuclei, G_i refers to the set of matched fragmented nuclei, and S_k corresponds to the set of fragmented nuclei that do not match any segmented nuclei [35,8]. The AJI metric is a crucial measure for evaluating segmentation performance, as it is more robust in penalizing incorrect segmentation predictions compared to other metrics, making it a reliable indicator of segmentation accuracy [8].

5. DETAILS OF THE SYSTEM

In the proposed LinkNet model supported by a VGG16 backbone for nuclear segmentation, the convolutional blocks in the encoder part of the LinkNet segmentation model have been replaced with the blocks from the VGG16 model. Figure 2 presents the architecture of the developed model in this study.

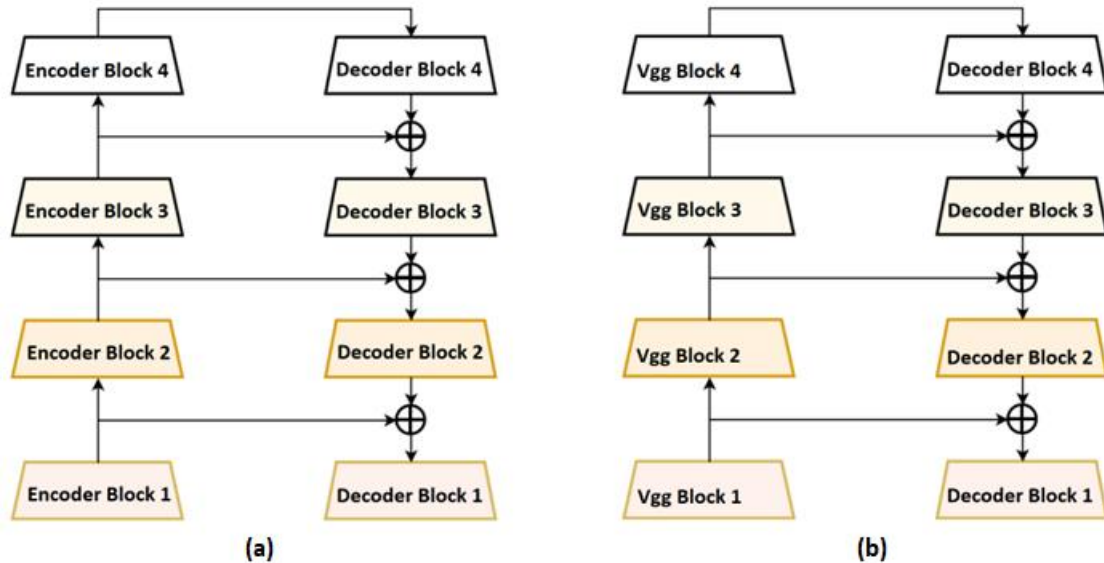


Fig 2. LinkNet Model Architecture Supported by a VGG16 Backbone (a) Original LinkNet Model, (b) LinkNet Model Supported by a VGG16 Backbone.

The proposed segmentation model is an enhanced version of the original LinkNet architecture, incorporating a VGG16 backbone in place of the standard LinkNet encoder. The original LinkNet model consists of four encoder blocks and four decoder blocks, where the encoder progressively extracts hierarchical features from the input image through convolutional operations, batch normalization, and activation functions. In this process, the spatial resolution of the feature maps is reduced while the number of feature channels increases. The decoder section, in turn, restores the resolution through upsampling, utilizing skip connections that retain fine-grained spatial details to improve segmentation accuracy.

In the modified model, the encoder component of LinkNet is replaced with the convolutional blocks of VGG16 to enhance feature extraction capabilities. Specifically, the first encoder block of LinkNet is substituted with VGG16 Block 1, while VGG16 Block 2 replaces the second encoder block. The third and fourth encoder blocks of LinkNet are replaced with the combined structure of VGG16 Blocks 3 and 4, and the final encoder block is substituted with VGG16 Block 5. The integration of VGG16 as the feature extractor allows for deeper and more refined hierarchical feature representation, enabling the model to better capture both low-level textures and high-level semantic structures within an image. The decoder section of the model retains the original LinkNet structure, where each decoder block progressively upsamples the extracted features and refines the segmentation mask, leveraging skip connections for improved spatial detail retention.

The main advantage of using a VGG16-backed LinkNet model is its improved capacity to capture complex structural features, which is particularly beneficial for nuclear segmentation tasks. The deep convolutional layers of VGG16 facilitate robust feature representation, contributing to improved segmentation accuracy. Additionally, the model benefits from pre-trained VGG16 weights, which improve generalization when applied to diverse datasets. The

presence of skip connections ensures that the detailed features extracted in the earlier layers of VGG16 are effectively incorporated during the upsampling process, leading to more precise boundary delineation in segmented images. By integrating VGG16 into the LinkNet framework, the proposed model achieves a balance between computational efficiency and segmentation accuracy. The hierarchical structure of VGG16 provides strong feature extraction capabilities, while the efficient upsampling mechanism of LinkNet maintains the model’s ability to generate high-resolution segmentation masks. This combination renders the proposed approach well-suited to complex segmentation tasks, such as nuclei segmentation in histopathological images, where fine structural details play a crucial role in analysis and interpretation.

6. RESULTS AND DISCUSSION

6.1. Parameter Settings

Experimental studies were performed with NVIDIA RTX 4070 8GB GPU resource. Tensorflow version 2.15.0 was preferred in the study and was run using 0.0001 learning rate and Adam optimizer for 100 epochs on Jupyter Notebook.

6.2 Experimental Results

Table 3 presents the literature results obtained using the CryoNuSeg dataset, along with the results achieved by the proposed model in this study. The best-performing results for each performance metric are highlighted in bold. Additionally, Figure 3 provides a visual representation of test images processed using the proposed model, demonstrating its segmentation performance.

Upon examining the comparative results in Table 3, it is evident that studies conducted using the CryoNuSeg dataset have employed state-of-the-art deep learning models in the encoder components of segmentation architectures [36-37].

The key distinction of the proposed method from similar and previous studies lies in its focus on the encoder model rather than the segmentation model itself it focuses on the encoder model instead of focusing on the segmentation model. This is because the results in Table 3 show that studies using the U-Net model developed for medical image segmentation are predominant. In this study, after a simple data augmentation preprocessing, the LinkNet model supported by the Vgg16 backbone achieved the highest AJI score in the literature. Achieving the highest score with the AJI metric, which is quite ruthless in penalizing incorrectly matched or incorrectly predicted kernels in segmentation tasks, demonstrates the effectiveness of the proposed model in nuclei segmentation.

Table 3. Results of Studies with CryoNuSeg Dataset

Model	DS	F1 Score	IoU	AJI
Two-Stage U-Net [36]	0.803	-	-	0.525
Nested U-Net backed by EfficientNet backbone [35]	0.929	-	-	0.604
CNN encoder-based U-Net [38]	0.815	-	-	0.541
EfficientNetv2 and the Attention Module [37]	0.941	-	-	0.605
U-Net based on Recurrent Neural Networks [39]	0.820	-	0.697	-
DONSeg [40]	0.672	-	-	0.441
UN-SAM [41]	0.804	0.807	0.652	-
MDLA-Unet [42]	0.807	-	-	-
Light-weight multi-scale attention [43]	0.810	-	0.685	-
LinkNet supported by Vgg16 backbone	0.840	0.845	0.731	0.731

The LinkNet model supported by the proposed VGG16 backbone for nuclei segmentation demonstrated remarkable performance, surpassing the results of multiple previous studies, including those conducted by the creators of the CryoNuSeg dataset [29, 38]. This superior performance can be attributed to several critical factors that merit further discussion.

First and foremost, the integration of a robust, multi-parameter deep learning architecture like VGG16 in the encoder component of the LinkNet model proved to be highly effective. VGG16's hierarchical structure, with its ability to capture both low-level features in initial blocks and high-level semantic information in deeper layers, enabled comprehensive feature extraction from histopathological images. This dual capability is particularly crucial for nuclei segmentation, where both textural details and structural context significantly influence segmentation accuracy. The experimental results, as evidenced by the highest AJI score (0.731) among comparable studies, validate the efficacy of this architectural decision.

A key methodological contribution of this work was the emphasis on enhancing the encoder component rather than focusing exclusively on modifying the segmentation architecture itself. Most previous studies utilizing the CryoNuSeg dataset have primarily concentrated on adapting the U-Net architecture, which has been the de facto standard for medical image segmentation. Our approach diverged from this trend by implementing LinkNet with a VGG16 backbone, demonstrating that alternative segmentation architectures can achieve superior results when paired with appropriate feature extractors. This finding suggests that the choice of encoder may have a more substantial impact on segmentation performance than the underlying segmentation framework, especially for complex tasks like nuclei segmentation in histopathological images.

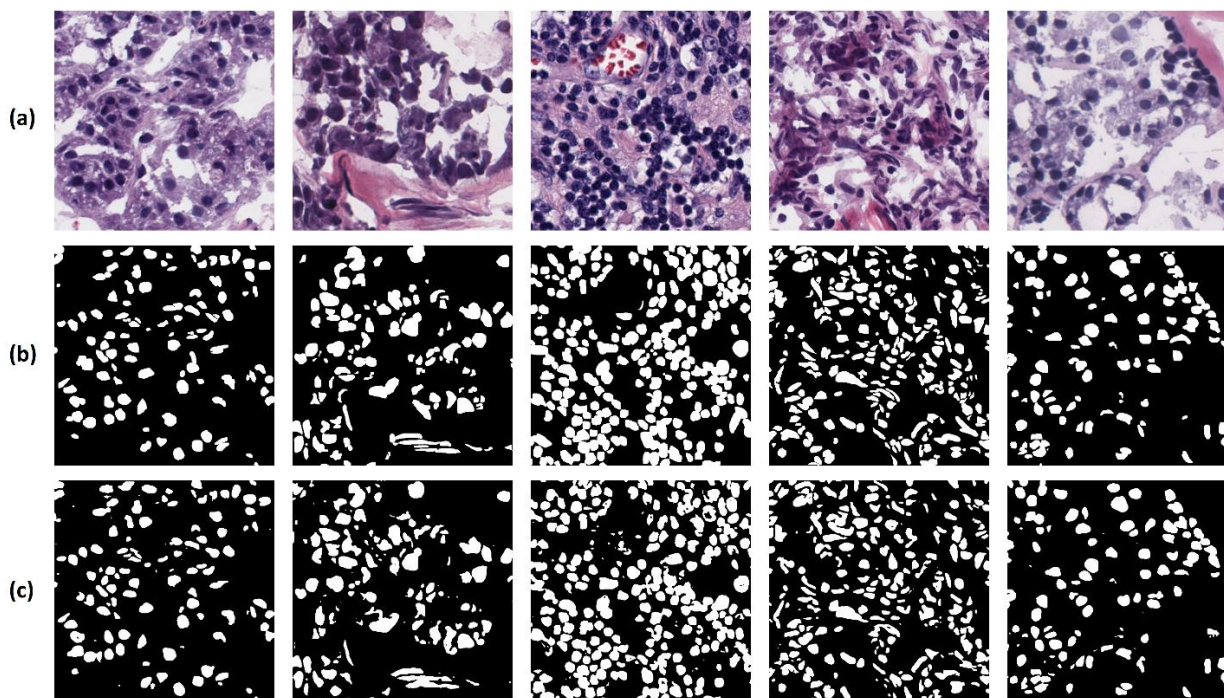


Fig 3. Running the CryoNuSeg dataset with the proposed model (a) Original histopathological input images, b) Ground truth segmentation masks annotated by experts, c) Predicted segmentation masks generated by the proposed LinkNet model supported by VGG16 backbone

The data preprocessing stage, particularly the application of data augmentation techniques, played a vital role in the model's success. Despite the relatively small size of the CryoNuSeg dataset (only 30 original images), our augmentation strategy expanded the training set to 1,000 images, significantly enhancing data diversity. This approach mitigated potential overfitting issues that often plague deep learning models trained on limited datasets. The combination of flipping and cropping techniques introduced variations in orientation and scale, enabling the model to learn more robust and generalizable features. This comprehensive preprocessing approach contrasts with some previous studies that utilized more limited augmentation techniques or none at all.

It is particularly noteworthy that our model achieved the highest score on the AJI, a metric known for its stringent evaluation of segmentation accuracy by severely penalizing incorrectly matched or predicted nuclei. AJI provides a more rigorous assessment of instance-level segmentation performance compared to pixel-level metrics like Dice Score

or IoU. Our model’s superior performance on this challenging metric underscores its effectiveness in correctly identifying individual nuclei boundaries, a critical requirement for practical applications in histopathological analysis and clinical decision support.

The symmetric two-stage architecture of segmentation models, comprising encoder and decoder components, allows for an interesting analysis of feature learning dynamics. In our approach, the VGG16 backbone in the encoder fulfilled a dual function: extracting low-level textural features in the initial blocks and high-level contextual features in the deeper blocks. This hierarchical feature extraction, when coupled with LinkNet’s efficient decoder pathway, facilitated precise boundary delineation of nuclei in histopathological images. The skip connections between encoder and decoder blocks further enhanced the model’s ability to preserve fine spatial details while incorporating contextual information, resulting in more accurate segmentation masks.

Despite these achievements, there remain several limitations and opportunities for future research. First, although our model showed superior performance on the CryoNuSeg dataset, its generalizability to other histopathological datasets with different staining protocols or tissue types requires further investigation. Second, the computational complexity of the VGG16 backbone, while justified by its performance benefits, may pose challenges for deployment in resource-constrained environments.

Future research directions could explore several promising avenues. The evaluation of alternative combinations of segmentation frameworks and backbone architectures could yield further improvements or identify optimal pairings for specific histopathological applications. More recent architectures such as EfficientNet, Vision Transformers, or hybrid models could potentially enhance feature extraction while reducing computational demands. Additionally, hyperparameter optimization of the backbone models, particularly learning rates and regularization strategies, could further refine segmentation performance. Advanced data augmentation techniques, such as style transfer or adversarial training, might further improve model robustness to variations in staining and imaging conditions commonly encountered in clinical settings.

Another promising direction involves the incorporation of attention mechanisms specifically designed for histopathological image analysis, which could enhance the model’s focus on relevant nuclear structures while suppressing background noise. Additionally, exploring multi-task learning approaches that simultaneously perform nuclei segmentation and classification could provide more comprehensive analytical capabilities for pathological assessment.

Table 4 shows the evaluation results of the proposed method on the CPM-17 dataset. In order to fully evaluate the model success, the results of recent works conducted with the CPM-17 dataset are also included.

Table 4. Comparison recent works with CPM-17 dataset

Model	DCS	F1 Score	IoU	AJI
Mask2Former [44]	-	0.782	-	0.602
Rtmdet [45]	-	0.775	-	0.607
CACS [46]	0.751	-	-	0.546
Micro-Net [47]	0.857	-	-	0.661
HistoNeXt [48]	0.826	-	-	0.625
LinkNet supported by Vgg16 backbone	0.809	0.813	0.687	0.681

The evaluation of the proposed LinkNet supported by Vgg16 backbone model on the CPM-17 dataset offers critical insights into its generalizability across different histopathological domains. Although the model was exclusively trained on the CryoNuSeg dataset, it achieved highly competitive results on the CPM-17 test set, with an F1 Score of 0.813 and an AJI score of 0.681. These findings are particularly significant given the inherent differences between the two datasets in terms of tissue types, staining variability, and nuclei morphology. The consistency of performance across distinct datasets without additional fine-tuning indicates that the feature representations learned by the model are

robust and transferable, underscoring its potential applicability in real-world clinical settings where training data may be limited or heterogeneous.

This generalization capability highlights a major strength of the proposed approach, namely its architectural design that emphasizes rich and hierarchical feature extraction through the VGG16 backbone. While many existing models exhibit high accuracy within the scope of the training domain, they often fail to maintain performance when exposed to unseen data distributions. In contrast, our model demonstrates resilience against domain shift, suggesting that its encoder effectively captures nucleus-invariant characteristics that are preserved across datasets. This level of adaptability not only validates the architectural decisions made but also reinforces the relevance of encoder-focused design for histopathological segmentation tasks requiring strong cross-dataset generalization.

7. CONCLUSION

This study demonstrates that the LinkNet model supported by a VGG16 backbone provides an effective solution for nuclei segmentation in histopathological images. By prioritizing enhancements to the encoder component and implementing comprehensive data preprocessing, our approach achieved state-of-the-art performance on the CryoNuSeg dataset.

The success of this methodology highlights the importance of feature extraction capabilities in segmentation tasks and suggests that judicious selection of backbone architectures may be as critical as the choice of segmentation framework itself. These findings contribute valuable insights to the ongoing development of automated tools for histopathological image analysis, with potential applications in cancer diagnosis, prognosis, and personalized treatment planning.

ACKNOWLEDGMENT

The author gratefully acknowledges that a preliminary version of this paper appeared as an abstract in the IMISC2024 Conference Abstract Book.

ORCID

Furkan ATLAN  <https://orcid.org/0000-0003-1602-1941>

REFERENCES

- [1]. Van der Laak, J., Litjens, G., & Ciompi, F. (2021). Deep learning in histopathology: the path to the clinic. *Nature medicine*, 27(5), 775-784. <https://doi.org/10.1038/s41591-021-01343-4>
- [2]. Baidoshvili, A., Bucur, A., van Leeuwen, J., van der Laak, J., Kluin, P., & van Diest, P. J. (2018). Evaluating the benefits of digital pathology implementation: time savings in laboratory logistics. *Histopathology*, 73(5), 784-794. <https://doi.org/10.1111/his.13691>
- [3]. Zheng, Y., Li, J., Shi, J., Xie, F., Huai, J., Cao, M., & Jiang, Z. (2023). Kernel attention transformer for histopathology whole slide image analysis and assistant cancer diagnosis. *IEEE Transactions on Medical Imaging*, 42(9), 2726-2739. <https://doi.org/10.1109/TMI.2023.3264781>
- [4]. Barisoni, L., Lafata, K. J., Hewitt, S. M., Madabhushi, A., & Balis, U. G. (2020). Digital pathology and computational image analysis in nephropathology. *Nature Reviews Nephrology*, 16(11), 669-685. <https://doi.org/10.1038/s41581-020-0321-6>
- [5]. Martos, O., Hoque, M. Z., Keskinarkaus, A., Kemi, N., Näpänkangas, J., Eskuri, M., ... & Seppänen, T. (2023). Optimized detection and segmentation of nuclei in gastric cancer images using stain normalization and blurred artifact removal. *Pathology-Research and Practice*, 248, 154694. <https://doi.org/10.1016/j.prp.2023.154694>
- [6]. Yildirim, Z., Samet, R., Hancer, E., Nemati, N., & Mali, M. T. (2023). Gland Segmentation in H&E Histopathological Images using U-Net with Attention Module. *In 2023 Twelfth International Conference on Image Processing Theory, Tools and Applications (IPTA)*, 1-6. <https://doi.org/10.1109/IPTA59101.2023.10320014>

- [7]. Irshad, H., Veillard, A., Roux, L., & Racoceanu, D. (2013). Methods for nuclei detection, segmentation, and classification in digital histopathology: a review—current status and future potential. *IEEE reviews in biomedical engineering*, 7, 97-114. <https://doi.org/10.1109/RBME.2013.2295804>
- [8]. Hancer, E., Traore, M., Samet, R., Yildirim, Z., & Nemati, N. (2023). An imbalance-aware nuclei segmentation methodology for H&E stained histopathology images. *Biomedical Signal Processing and Control*, 83, 104720. <https://doi.org/10.1016/j.bspc.2023.104720>
- [9]. Verma, R., Kumar, N., Patil, A., Kurian, N. C., Rane, S., Graham, S., ... & Sethi, A. (2021). MoNuSAC2020: A multi-organ nuclei segmentation and classification challenge. *IEEE Transactions on Medical Imaging*, 40(12), 3413-3423. <https://doi.org/10.1109/TMI.2021.3085712>
- [10]. Long, J., Shelhamer, E., & Darrell, T. (2015). Fully convolutional networks for semantic segmentation. *In Proceedings of the IEEE conference on computer vision and pattern recognition*, 3431-3440.
- [11]. Ronneberger, O., Fischer, P., & Brox, T. (2015). U-net: Convolutional networks for biomedical image segmentation. *In Medical image computing and computer-assisted intervention—MICCAI 2015: 18th international conference*, 234-241. https://doi.org/10.1007/978-3-319-24574-4_28
- [12]. Zhou, Z., Rahman Siddiquee, M. M., Tajbakhsh, N., & Liang, J. (2018). Unet++: A nested u-net architecture for medical image segmentation. *In Deep Learning in Medical Image Analysis and Multimodal Learning for Clinical Decision Support: 4th International Workshop, DLMIA 2018, and 8th International Workshop, ML-CDS 2018, Held in Conjunction with MICCAI 2018*, 3-11. https://doi.org/10.1007/978-3-030-00889-5_1
- [13]. Çiçek, Ö., Abdulkadir, A., Lienkamp, S. S., Brox, T., & Ronneberger, O. (2016). 3D U-Net: learning dense volumetric segmentation from sparse annotation. *In Medical Image Computing and Computer-Assisted Intervention—MICCAI 2016: 19th International Conference*, 424-432. https://doi.org/10.1007/978-3-319-46723-8_49
- [14]. Abedalla, A., Abdullah, M., Al-Ayyoub, M., & Benkhelifa, E. (2020). The 2ST-UNet for pneumothorax segmentation in chest X-Rays using ResNet34 as a backbone for U-Net. *arXiv preprint arXiv:2009.02805*.
- [15]. Sharma, N., & Gupta, S. (2023). Semantic Segmentation of Gastrointestinal Tract using UNet Model with ResNet 18 Backbone. *In 2023 International Conference in Advances in Power, Signal, and Information Technology (APSIT)*, 226-230. <https://doi.org/10.1109/APSIT58554.2023.10201739>
- [16]. Das, N., & Das, S. (2024). Attention-UNet architectures with pretrained backbones for multi-class cardiac MR image segmentation. *Current Problems in Cardiology*, 49(1), 102129. <https://doi.org/10.1016/j.cpcardiol.2023.102129>
- [17]. Simonyan, K., & Zisserman, A. (2014). Very deep convolutional networks for large-scale image recognition. *arXiv preprint arXiv:1409.1556*.
- [18]. Chaurasia, A., & Culurciello, E. (2017). Linknet: Exploiting encoder representations for efficient semantic segmentation. *In 2017 IEEE visual communications and image processing (VCIP)*, 1-4. <https://doi.org/10.1109/VCIP.2017.8305148>
- [19]. Long, F. (2020). Microscopy cell nuclei segmentation with enhanced U-Net. *BMC bioinformatics*, 21(1), 8. <https://doi.org/10.1186/s12859-019-3332-1>
- [20]. Lal, S., Das, D., Alabhya, K., Kanfode, A., Kumar, A., & Kini, J. (2021). NucleiSegNet: Robust deep learning architecture for the nuclei segmentation of liver cancer histopathology images. *Computers in Biology and Medicine*, 128, 104075. <https://doi.org/10.1016/j.combiomed.2020.104075>
- [21]. Kumar, N., Verma, R., Anand, D., Zhou, Y., Onder, O. F., Tsougenis, E., ... & Sethi, A. (2019). A multi-organ nucleus segmentation challenge. *IEEE transactions on medical imaging*, 39(5), 1380-1391. <https://doi.org/10.1109/TMI.2019.2947628>
- [22]. Qin, J., He, Y., Zhou, Y., Zhao, J., & Ding, B. (2022). REU-Net: Region-enhanced nuclei segmentation network. *Computers in Biology and Medicine*, 146, 105546. <https://doi.org/10.1016/j.combiomed.2022.105546>
- [23]. Ahmad, I., Xia, Y., Cui, H., & Islam, Z. U. (2023). DAN-NucNet: A dual attention based framework for nuclei segmentation in cancer histology images under wild clinical conditions. *Expert Systems with Applications*, 213, 118945. <https://doi.org/10.1016/j.eswa.2022.118945>
- [24]. Li, Z., Tang, Z., Hu, J., Wang, X., Jia, D., & Zhang, Y. (2023). Nst: a nuclei segmentation method based on transformer for gastrointestinal cancer pathological images. *Biomedical Signal Processing and Control*, 84, 104785. <https://doi.org/10.1016/j.bspc.2023.104785>
- [25]. Goceri, E. (2024). Nuclei segmentation using attention aware and adversarial networks. *Neurocomputing*, 579, 127445. <https://doi.org/10.1016/j.neucom.2024.127445>

- [26]. Hasan, M. J., Ahmad, W. S. H. M. W., Fauzi, M. F. A., & Abas, F. S. (2024). Hybrid Deep Learning Architectures for Histological Image Segmentation. In *2024 International Conference on Artificial Intelligence in Information and Communication (ICAIIIC)*, 75-80. <https://doi.org/10.1109/ICAIIIC60209.2024.10463355>
- [27]. Hernández-García, A., & König, P. (2018). Data augmentation instead of explicit regularization. *arXiv preprint arXiv:1806.03852*.
- [28]. Vu, Q. D., Graham, S., Kurc, T., To, M. N. N., Shaban, M., Qaiser, T., ... & Farahani, K. (2019). Methods for segmentation and classification of digital microscopy tissue images. *Frontiers in bioengineering and biotechnology*, 7, 53. <https://doi.org/10.3389/fbioe.2019.00053>
- [29]. Mahbod, A., Schaefer, G., Bancher, B., Löw, C., Dorffner, G., Ecker, R., & Ellinger, I. (2021). CryoNuSeg: A dataset for nuclei instance segmentation of cryosectioned H&E-stained histological images. *Computers in biology and medicine*, 132, 104349. <https://doi.org/10.1016/j.compbiomed.2021.104349>
- [30]. Zhong, Z., Zheng, L., Kang, G., Li, S., & Yang, Y. (2020). Random erasing data augmentation. In *Proceedings of the AAAI conference on artificial intelligence*, 34(7), 13001-13008. <https://doi.org/10.1609/aaai.v34i07.7000>
- [31]. Ioffe, S., & Szegedy, C. (2015, June). Batch normalization: Accelerating deep network training by reducing internal covariate shift. In *International conference on machine learning*, 448-456.
- [32]. Nair, V., & Hinton, G. E. (2010). Rectified linear units improve restricted boltzmann machines. In *Proceedings of the 27th international conference on machine learning (ICML-10)*, 807-814.
- [33]. Nijaguna, G. S., Babu, J. A., Parameshachari, B. D., de Prado, R. P., & Frnda, J. (2023). Quantum Fruit Fly algorithm and ResNet50-VGG16 for medical diagnosis. *Applied Soft Computing*, 136, 110055. <https://doi.org/10.1016/j.asoc.2023.110055>
- [34]. Sun, J., Yang, F., Cheng, J., Wang, S., & Fu, L. (2024). Nondestructive identification of soybean protein in minced chicken meat based on hyperspectral imaging and VGG16-SVM. *Journal of Food Composition and Analysis*, 125, 105713. <https://doi.org/10.1016/j.jfca.2023.105713>
- [35]. Zhang, J., Li, C., Kosov, S., Grzegorzec, M., Shirahama, K., Jiang, T., ... & Li, H. (2021). LCU-Net: A novel low-cost U-Net for environmental microorganism image segmentation. *Pattern Recognition*, 115, 107885. <https://doi.org/10.1016/j.patcog.2021.107885>
- [36]. Le Dinh, T., Lee, S. H., Kwon, S. G., & Kwon, K. R. (2022). Cell nuclei segmentation in cryonuseg dataset using nested unet with efficientnet encoder. In *2022 International Conference on Electronics, Information, and Communication (ICEIC)*, 1-4. <https://doi.org/10.1109/ICEIC54506.2022.9748537>
- [37]. Liao, L., & Zhang, Z. (2023). Nuclear Segmentation Based on Recurrent Iteration and Fusion Attention Mechanism. In *2023 3rd International Conference on Electronic Information Engineering and Computer Science (EIECS)*, 365-371. <https://doi.org/10.1109/EIECS59936.2023.10435439>
- [38]. Mahbod, A., Schaefer, G., Dorffner, G., Hatamikia, S., Ecker, R., & Ellinger, I. (2022). A dual decoder u-net-based model for nuclei instance segmentation in hematoxylin and eosin-stained histological images. *Frontiers in Medicine*, 9, 978146. <https://doi.org/10.3389/fmed.2022.978146>
- [39]. Kadaskar, M., & Patil, N. (2023). Nuclei Segmentation using EfficientNetV2 and Convolutional Block Attention Module. In *2023 14th International Conference on Computing Communication and Networking Technologies (ICCCNT)*, 1-5. <https://doi.org/10.1109/ICCCNT56998.2023.10307210>
- [40]. Wang, Z., Zhang, Y., Wang, Y., Cai, L., & Zhang, Y. (2024). Dynamic Pseudo Label Optimization in Point-Supervised Nuclei Segmentation. *arXiv preprint arXiv:2406.16427*.
- [41]. Chen, Z., Xu, Q., Liu, X., & Yuan, Y. (2024). UN-SAM: Universal Prompt-Free Segmentation for Generalized Nuclei Images. *arXiv preprint arXiv:2402.16663*.
- [42]. Sun, X., Li, S., Chen, Y., Chen, J., Geng, H., Sun, K., ... & Zhang, H. (2025). Multiple Differential Convolution and Local-Variation Attention UNet: Nucleus Semantic Segmentation Based on Multiple Differential Convolution and Local-Variation Attention. *Electronics*, 14(6), 1058. <https://doi.org/10.3390/electronics14061058>
- [43]. Zhang, X., Xu, J., He, D., Wang, K., & Wang, L. (2025). Lightweight multi-scale attention group fusion structure for nuclei segmentation. *The Journal of Supercomputing*, 81(1), 199. <https://doi.org/10.1007/s11227-024-06710-9>
- [44]. Cheng, B., Misra, I., Schwing, A. G., Kirillov, A., & Girdhar, R. (2022). Masked-attention mask transformer for universal image segmentation. In *Proceedings of the IEEE/CVF conference on computer vision and pattern recognition* (pp. 1290-1299).
- [45]. Lyu, C., Zhang, W., Huang, H., Zhou, Y., Wang, Y., Liu, Y., ... & Chen, K. (2022). Rtmdet: An empirical study of designing real-time object detectors. *arXiv preprint arXiv:2212.07784*. arXiv preprint arXiv:2212.07784 2022

- [46].Ruan, H. (2024, December). A Color-Aware Unsupervised Segmentation Network for Nuclei in Histopathology Images. In *2024 4th International Conference on Electronic Information Engineering and Computer Communication (EIECC)* (pp. 627-631). IEEE. <https://doi.org/10.1109/EIECC64539.2024.10929140>
- [47].Raza, S. E. A., Cheung, L., Shaban, M., Graham, S., Epstein, D., Plantaris, S., ... & Rajpoot, N. M. (2019). Micro-Net: A unified model for segmentation of various objects in microscopy images. *Medical image analysis*, 52, 160-173. <https://doi.org/10.1016/j.media.2018.12.003>
- [48].Chen, J., Wang, R., Dong, W., He, H., & Wang, S. (2025). HistoNeXt: dual-mechanism feature pyramid network for cell nuclear segmentation and classification. *BMC Medical Imaging*, 25(1), 9. <https://doi.org/10.1186/s12880-025-01550-2>

Techno-Science Paper ID:1658832